JOURNAL OF AIRCRAFT
Vol. 48, No. 4, July–August 2011

Engineering Notes

Investigating Negative Drag in Grid Convergence for Two-Dimensional Euler Solutions

Daniel Destarac*
ONERA, 92190 Meudon, France

DOI: 10.2514/1.C031330

Introduction

VASSBERG and Jameson [1] pursue grid convergence of two-dimensional Euler solutions for subcritical and transonic, nonlifting and lifting, flow conditions, with and without point-vortex correction applied to the far-field boundary condition. It may be remarked that tables relative to the subcritical cases contain some negative values of pressure drag. A hypothesis on the origin of this oddity is proposed in this Note.

Purpose

Of the different test cases considered in [1], only the subcritical lifting one ($M_\infty = 0.5$ and $\alpha = 1.25°$) will be discussed here. Theoretical pressure drag is zero. Only solutions computed with point-vortex correction at the far-field boundary will be considered. (It is shown in [2] that zero pressure drag cannot be attained in the absence of this correction with the grids used in [1].)

Vassberg and Jameson's [1] grids have an identical number of cells (nc) of aspect ratio 1 in the two directions of an O-type topology, thus avoiding a difficulty mentioned by Salas in [3]. In Fig. 1 pressure drag is plotted (with spline fit) against the conventional measure $1/\mathrm{nc}$ of grid refinement, for solutions from [1] obtained with the FLO82-HCUSP [4] and CFL3D [5] codes and for solutions computed in view of the present Note with the ONERA CANARI code [6] (Vassberg and Jameson's [1] grids having been kindly supplied to ONERA). Pressure drag from CFL3D has a monotone evolution toward zero from the positive side, a behavior familiar to anyone involved in computational fluid dynamics. But drag computed with either FLO82-HCUSP or CANARI, while also giving positive drag for the lowest grid refinement levels, becomes negative with grid refinement and finally tends toward zero from the negative side.

The purpose of this Note is to try to explain why negative drag has not been observed since numerical resolution of the Euler equations has reached some maturity, as well as its origin in the present case.

Hypothesis

Figure 2 compares a Vassberg and Jameson [1] grid and a grid typical of the practice of, say, 20 years ago in solving the Euler equations. These grids are quite different because they were designed for different purposes. Vassberg and Jameson's grids are perfect for accuracy studies. The bottom grid in Fig. 2 has obviously been designed with the objective of minimizing the number of cells for a given level of expected accuracy of the solution; there are more cells along the airfoil than normal to it (to minimize spurious entropy productions), and the strong stretching aims at refining the grid near the wall, normal to it (to improve the accuracy of the boundary condition).

Now let us try drag grid convergence with a series of such typical highly stretched grids. The CANARI code is used with the same numerical ingredients and parameters as with Vassberg and Jameson's [1] grids. The results are plotted in Fig. 3. The grid refinement measure, $1/\sqrt{\mathrm{nc}i \times \mathrm{nc}j}$, where i, and j denote the two grid topological directions, reduces to the previous $1/\mathrm{nc}$ when $\mathrm{nc}i = \mathrm{nc}j$. We now obtain monotone positive drag, at least in the investigated interval of refinement.

Let us make the likely hypothesis that artificial dissipation in the field produces essentially positive drag and the more hazardous one that the boundary condition at the wall has an antidissipative property. Then we would, as it were, have been missing negative drag all these years, because the usual local grid refinement normal to the wall, with strongly "flattened" cells, made the field-dissipation effect dominant over that of the boundary condition. And it would appear now because Vassberg and Jameson's [1] grids, having a cell aspect of one, change the relative importance of the two phenomena for very high refinement levels; streamwise refinement (mostly) will extinguish the effect of field dissipation before normal refinement (mostly) extinguishes that of the boundary-condition antidissipation.

In Fig. 4, a sketch inspired by the qualitatively similar behavior of FLO82-HCUSP and CANARI in Fig. 1 illustrates this interpretation.

Numerical Tests

The next step in this study is to act separately on the two hypothetical causes, wall-slip boundary condition and artificial field dissipation.

In the CANARI code, the discretization is cell-centered. In the case of the Euler equations, pressure at a wall-slip boundary can be computed through multidirectional extrapolation [7], which involves the cell metrics and pressure at the centers of the cell and of the neighboring ones. This is the option used in the above-discussed computations. A cruder monodirectional index-based extrapolation technique is available for cases where poor grid quality may induce negative pressure. Drag grid convergence with Vassberg and Jameson's [1] grids with the two options is compared in Fig. 5. The results with the monodirectional extrapolation, positive drag, strong monotone evolution, may be interpreted as the consequence of a

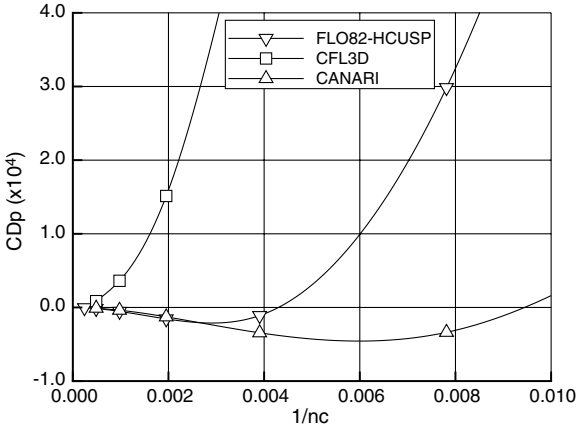

Fig. 1 Grid convergence of pressure drag (nc denotes the equal number of cells in the two directions) with Vassberg and Jameson's [1] NACA0012 grids ($M_\infty = 0.50$, $\alpha = 1.25°$). FLO82-HCUSP and CFL3D results are from [1].

Received 30 November 2010; revision received 17 March 2011; accepted for publication 29 March 2011.

*Engineer, Applied Aerodynamics Department; daniel.destarac@onera.fr.

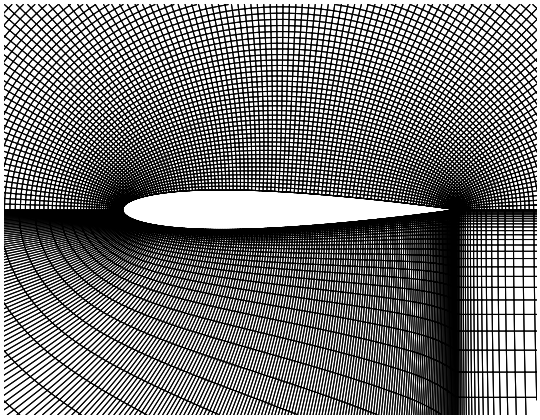

Fig. 2 Two types of grids: Vassberg and Jameson's [1] high-quality O grid (256 × 256 cells; top) and typical grid used for solving the Euler equations 20 years ago (512 × 64 cells; bottom).

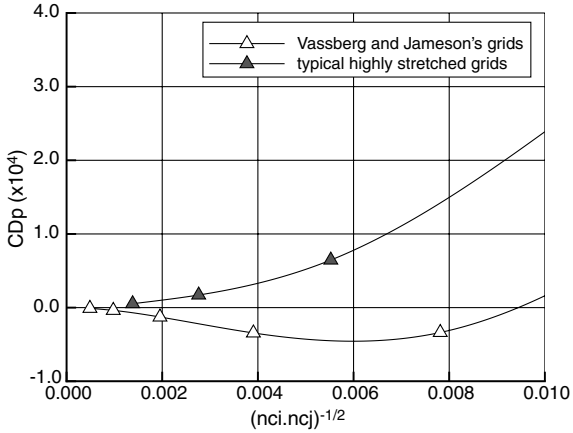

Fig. 3 Grid convergence of pressure drag (n*ci*, n*cj*: numbers of cells) for Vassberg and Jameson's [1] grids vs typical highly stretched grids. CANARI computations (NACA0012, $M_\infty = 0.50$, and $\alpha = 1.25°$).

dissipative or nondissipative boundary condition instead of an antidissipative one.

In regard to artificial dissipation, CANARI, which has a centered scheme, uses Jameson's blend of second and fourth differences. Standard values for the parameters monitoring these terms, $k2 = 0.25$ and $k4 = 0.008$, have been used in the computations previously discussed. In subcritical flow, $k2$ may be set to zero. Also in subcritical (only) and two-dimensional flow (at least), the effect of $k4$

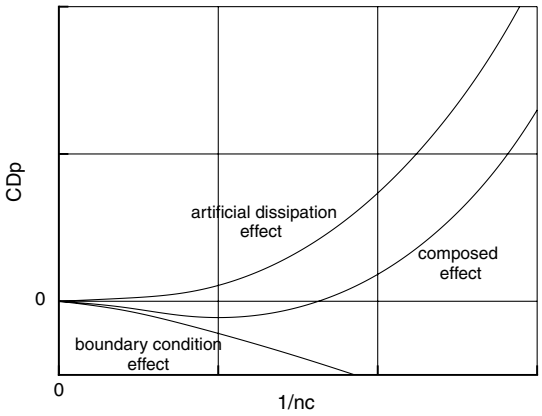

Fig. 4 Composition of two postulated effects on pressure drag in certain solutions to the Euler equations: artificial dissipation in the field and antidissipative wall-slip boundary condition.

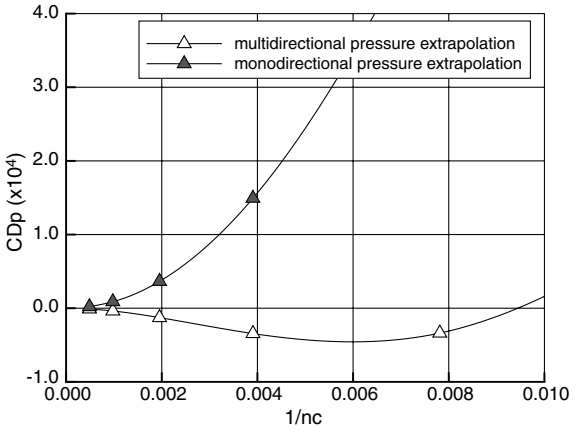

Fig. 5 Grid convergence of pressure drag (nc denotes the equal number of cells in the two directions) with wall-slip boundary-condition option effect for Vassberg and Jameson's [1] grids and CANARI computations (NACA0012, $M_\infty = 0.50$, and $\alpha = 1.25°$).

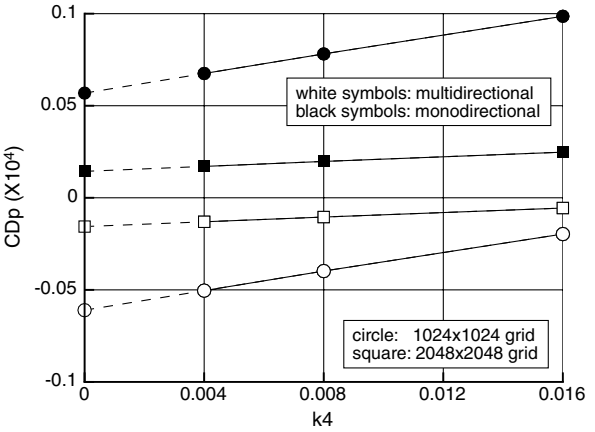

Fig. 6 Extrapolation of pressure drag to zero dissipation ($k2 = 0$ and $k4 \to 0$) with monodirectional and multidirectional pressure extrapolation for Vassberg and Jameson's [1] grids and CANARI computations (NACA0012, $M_\infty = 0.50$, and $\alpha = 1.25°$).

on pressure drag is quasi-linear. It is thus possible to extrapolate pressure drag to zero dissipation, as shown in Fig. 6 for the two finest grid levels and both pressure extrapolations to the wall. In Fig. 7, grid convergence of pressure drag is plotted with such extrapolated to

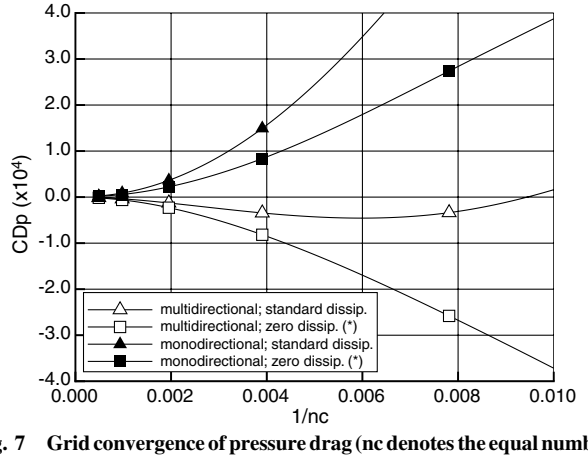

Fig. 7 Grid convergence of pressure drag (nc denotes the equal number of cells in the two directions) with artificial dissipation effect for two different wall-slip boundary conditions (* denotes extrapolated) for Vassberg and Jameson's [1] grids and CANARI computations (NACA0012, $M_\infty = 0.50$, and $\alpha = 1.25°$).

zero dissipation data, and with the standard dissipation data of Fig. 5. With zero dissipation, grid convergence of pressure drag with multidirectional pressure extrapolation becomes monotone, approximately symmetrical (negative-drag side) to that with monodirectional extrapolation (positive-drag side).

It is somewhat disappointing that multidirectional extrapolation, using more information, do not give more accurate results than monodirectional extrapolation. But Fig. 7 confirms the hypothesis illustrated by Fig. 4. Of the two boundary treatments, one is dissipative and the other is antidissipative. Negative drag is obtained when the antidissipative effect of the boundary condition dominates over that of artificial field dissipation.

Conclusions

In two-dimensional solutions of the Euler equations in subcritical flow, pressure drag, which should theoretically be zero, is known to be usually positive (spurious drag). However, negative values may also be obtained. This occurs when an antidissipative effect of a wall boundary condition dominates over the artificial field dissipation. Such a behavior was made apparent in a recent paper with cells of aspect ratio 1, which do not damp the boundary-condition effect as do usual stretched grids with flattened cells near the wall.

References

[1] Vassberg, J. C., and Jameson, A., "In Pursuit of Grid Convergence for Two-Dimensional Euler Solutions," *Journal of Aircraft*, Vol. 47, No. 4, July–Aug. 2010, pp. 1152–1166. doi:10.2514/1.46737

[2] Destarac, D., "Spurious Far-Field-Boundary Induced Drag in Two-Dimensional Flow Simulations," *Journal of Aircraft*, Vol. 48, No. 4, 2011, pp. 1444–1455. doi:10.2514/1.C031331

[3] Salas, M. D., "Some Observations on Grid Convergence," *Computers and Fluids*, Vol. 35, 2006, pp. 688–692. doi:10.1016/j.compfluid.2006.01.003

[4] Jameson, A., "Artificial Diffusion, Upwind Biasing, Limiters and their Effect on Accuracy and Multigrid Convergence in Transonic and Hypersonic Flow," 11th AIAA Computational Fluid Dynamics Conference, AIAA Paper 93-3359, Orlando, FL, July 1993.

[5] Krist, S. L., Biedron, R. T., and Rumsey, C. L., "CFL3D User's Manual, Version 5.0" NASA NASA-TM 1998-208444, June 1998.

[6] Couaillier, V., "Numerical Simulation of Separated Turbulent Flows Based on the Solution of RANS/Low Reynolds Two-Equation Model," 37th Aerospace Science Meeting and Exhibit, AIAA Paper 99-154, Reno, NV, 11–14 Jan. 1999.

[7] Couaillier, V., and Delbos, M., "Accurate Boundary Conditions with Classical and Higher Order CFD Methods," *RTO Applied Vehicle Technology Panel Symposium*, RTO-MP-AVT-147, NATO Research and Technology Organisation, Paper 29, 3–6 Dec. 2007.